Proceedings of the 30th International Conference on Ocean, Offshore, and Arctic Engineering
OMAE2011
June 19-24, 2011, Rotterdam, The Netherlands

OMAE2011-49863

DEVELOPMENT AND VERIFICATION OF A COMPUTATIONAL FLUID DYNAMICS MODEL OF A HORIZONTAL-AXIS TIDAL CURRENT TURBINE

Michael J. Lawson *
National Renewable Energy Laboratory
National Wind Technology Center
Golden, CO 80401
Email: michael.lawson@nrel.gov

Ye Li
National Renewable Energy Laboratory
National Wind Technology Center
Golden, CO 80401
Email: ye.li@nrel.gov

Danny C. Sale
University of Washington
Mechanical Engineering Deaprtment
Seattle, WA 98195
Email: sale.danny@gmail.com

ABSTRACT

This paper describes the development of a computational fluid dynamics (CFD) methodology to simulate the hydrodynamics of horizontal-axis tidal current turbines (HATTs). First, an HATT blade was designed using the blade element momentum method in conjunction with a genetic optimization algorithm. Several unstructured computational grids were generated using this blade geometry and steady CFD simulations were used to perform a grid resolution study. Transient simulations were then performed to determine the effect of time-dependent flow phenomena and the size of the computational timestep on the numerical solution. Qualitative measures of the CFD solutions were independent of the grid resolution. Conversely, quantitative comparisons of the results indicated that the use of coarse computational grids results in an under prediction of the hydrodynamic forces on the turbine blade in comparison to the forces predicted using more resolved grids. For the turbine operating conditions considered in this study, the effect of the computational timestep on the CFD solution was found to be minimal, and the results from steady and transient simulations were in good agreement. Additionally, the CFD results were compared to corresponding blade element momentum method calculations and reasonable agreement was shown. Nevertheless, we expect that for other turbine operating conditions, where the flow over the blade is separated, transient simulations will be required.

*Address all correspondence to this author.

INTRODUCTION

The kinetic energy available within tidal currents is an untapped source of renewable energy. If a cost-effective method of capturing this energy can be developed, tidal currents could be harnessed to help satisfy the world's growing energy needs. Horizontal-axis tidal current turbines (HATTs) are one promising technology that is being developed for this purpose [1].

HATTs operate using the same mechanical principles as wind turbines. At their most basic, HATTs convert kinetic energy within a tidal stream into electricity. Several companies have developed HATTs with the intent of commercializing the technology. Two examples are Marine Current Turbine's twin-rotor SeaGen that is undergoing testing off the coast of Northern Ireland, and Verdant Power's single rotor turbine that has been deployed successfully in the East River near New York City.

The ability to design efficient HATT blades and accurately predict their performance is critical for the success of the tidal current turbine industry. Traditionally, reduced order numerical methods, such as the blade element momentum method and the vortex element method, have been used to design and predict the performance of wind turbine blades. Batton et al. [2, 3] and Baltazar et al. [4,5] recently demonstrated that these methods can also be employed to characterize HATT blade performance. In both cases, results from the numerical simulations were shown to be in good agreement with experimental measurements of an HATT made by Bahaj et al. [6, 7].

Nevertheless, it is important to note that the blade element momentum method and the boundary element method rely on experimental measurements and empirical correlations to achieve

accurate results. For example, blade element momentum calculations use compiled experimental data to estimate the hydrodynamic forces on the blade, whereas boundary element methods typically employ empirical correlation to account for far-field wake effects. Unfortunately, neither method inherently models the effects of viscosity, which need to be considered to achieve the most accurate turbine performance predictions possible.

Conversely, computational fluid dynamics (CFD) simulations of the Navier-Stokes equations model fluid flows starting from first principles, and therefore inherently capture viscous effects. In the last decade, CFD models of wind turbines have been used to accurately reproduce experimental results (e.g. [8–12]) and have been used extensively to study complex flow phenomena that have not been quantifiable through the use of simplified numerical methods. Given the successful use of CFD in the wind industry, it is practical to utilize CFD tools to advance HATT technology.

Objective

The objective of this study is to develop a CFD methodology to simulate HATTs and to determine the effects of computational grid resolution and computational timestep on the accuracy of the simulations. First, we used the blade element momentum method in conjunction with a genetic optimization algorithm to design an HATT blade. Using this blade geometry, several CFD simulations were performed using computational grids with successively finer spatial resolution. Finally, transient simulations were performed to determine if temporal effects must be considered to make accurate predictions of HATT performance. CFD predictions of turbine rotor torque and blade root flap moment were also compared to corresponding blade element momentum calculations. It is noted that the CFD model only includes the turbine blade and hub geometries. Other turbine components, such as the tower and nacelle, were not considered in this preliminary study.

TURBINE BLADE DESIGN

Specifications and operating conditions

In this paper we consider a hypothetical 550 KW turbine intended for deployment in the Northern Admiralty Inlet of Puget Sound in Washington State. An acoustic Doppler current profiler survey at this site [13] shows the mean water velocity is approximately 1 m/s, although velocities as high as 3 m/s occur during the tidal cycle.

The design and operating specifications for the turbine are presented in Tab. 1. The turbine considered in this study had a 20 m diameter rotor comprised of a 2 m diameter hub and two 9 m blades. The blade design was optimized for a variable-speed variable-pitch (VSVP) turbine with a maximum rotation rate of 11.5 rpm. A NACA 63(1)-424 airfoil was chosen as the primary shape for the turbine blade. A NACA 63-series blade was selected because the minimum pressure coefficient is relatively large, which makes this airfoil resistant to cavitation. Additionally, the NACA 63-series blades were an attractive choice for the current application because they are known to delay stall and are less sensitive to leading edge roughness than the NACA 4- and 5-series airfoils.

TABLE 1. TURBINE SPECIFICATIONS.

No. of blades	2
Primary blade airfoil	NACA 63_1-424
Rated power (kW)	550
Control	Variable-speed variable-pitch
Rotor diameter (m)	20
Hub diameter (m)	2
Max. rotor speed (rpm)	11.5
Flow speeds (m/s)	0.5-3.0
Hub height (m)	18
Water depth (m)	33

Given that the blade design was intended for a VSVP turbine, we assumed a circular cross-section at the blade root (to allow for a blade-pitching mechanism) that transitioned to the NACA 63(1)-424 airfoil shape at 20% of the blade span. It may be possible to improve the performance of the blade (i.e. increase power generation) by using several different airfoil shapes to define the blade geometry. Future studies will be performed to explore this possibility.

Blade optimization

We used our recently developed numerical tool, Harp_Opt [14], to conduct the basic turbine blade design. Harp_Opt is the combination of the blade element moment code WT_Perf [15] with a genetic algorithm to optimize the blade twist angle and chord length distribution along the span. Harp_Opt has been widely used by industry and academia to study HATTs.

The optimization objective for the blade design process was to maximize power generation over a range of flow speeds from 0.5 m/s to 3.0 m/s. Within this range of flow speeds, Harp_Opt determined the rotor's rotation speed and the blade's pitch angle. The optimization algorithm bounded the turbine's maximum power output at 550 kW and also avoided cavitation. Specifically, cavitation was avoided by comparing the minimum pressure over the blade to the fluid vapor pressure and avoiding blade designs and turbine operating conditions for which cavitation is likely. XFOIL was used to predict the NACA 63(1)-424 airfoil's lift, drag, and pressure coefficients used for the blade element momentum analysis.

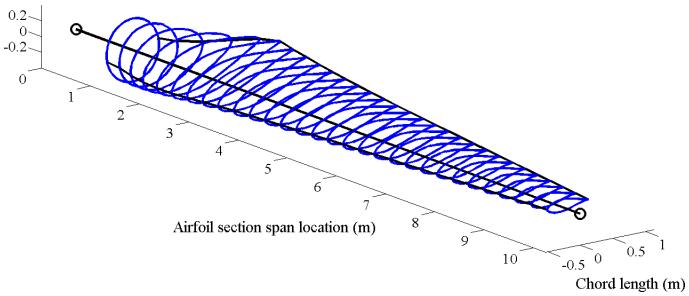

FIGURE 1. THREE-DIMENSIONAL REPRESENTATION OF THE TURBINE BLADE DESIGNED USING Harp_Opt.

Figure 1 presents an image of the blade and Fig. 2 summarizes turbine operating conditions determined by Harp_Opt. The WT_Perf blade element momentum calculations show that the angle of attack for the blade was well below the stall angle across the entire blade span for all operating conditions. Thus the flow over the blade was expected to remain fully attached under normal operating conditions.

CFD METHODOLOGY

CFD simulations predict the motion of a fluid within a given domain by discretizing the governing Navier-Stokes equations and solving the resulting set of algebraic equations. The remainder of this paper describes the development and verification of a CFD methodology to quickly and accurately simulate the performance of an HATT.

Assumptions

The CFD model assumed that the density of sea water was constant and that the flow was free of cavitation (in accordance with the Harp_Opt design). Additionally, the effects of gravity were neglected in the CFD simulations, which affectively rendered the blade neutrally buoyant. Future CFD simulations could be easily adapted to include gravitational forces, thus allowing the effects of buoyancy and cavitation to be studied.

Turbulence modeling

The k-ω SST (shear stress transport) Reynolds-averaged Navier-Stokes (RANS) sub-grid scale model [16] was used to simulate turbulence in the flow. The k-ω SST model was selected because it has been successfully used to simulate turbulent flow over airfoils. Additionally, several CFD studies of wind turbines (e.g. [8–12, 17, 18]) have successfully used the k-ω SST model to make numerical predictions of turbine performance. A few of these studies (e.g. [8–12]) have shown good agreement with experimental measurements [19].

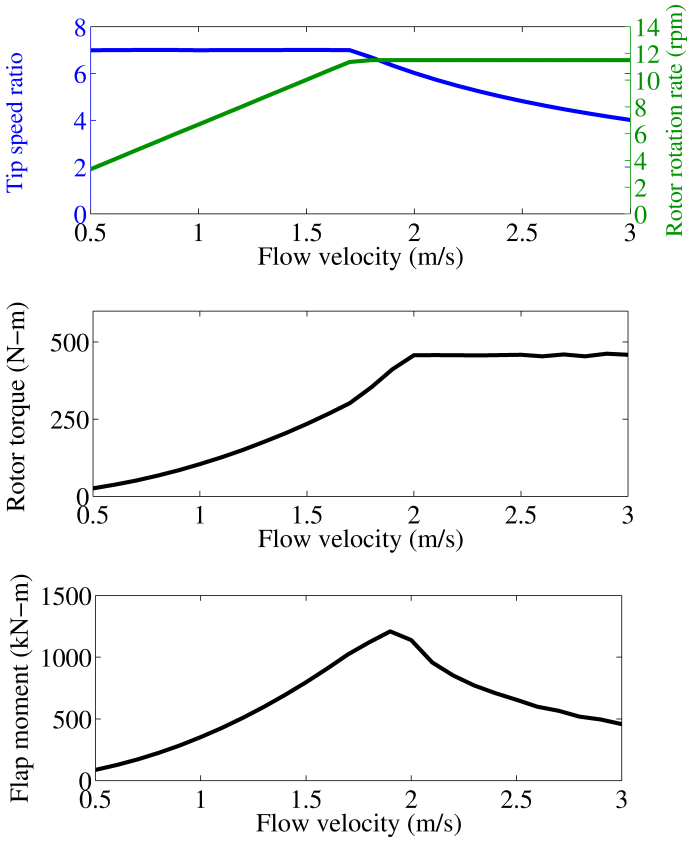

FIGURE 2. TURBINE OPERATING CONDITIONS DETERMINED USING Harp_Opt.

Computational domain and boundary conditions

We took advantage of the 180 degree periodicity of the two-bladed rotor and only simulated one blade and half of the hub. Accordingly, the computational domain consisted of a single turbine blade and half of the hub placed in a large half-cylinder with a periodic boundary condition applied across the bottom of the domain as shown in Fig. 3. The domain was separated into two subdomains to facilitate simulating the rotation of the rotor. One subdomain contained the grid elements surrounding the rotor and those in the wake region (referred to as the rotor domain), while the other subdomain contained the cells in the outer region (referred to as the outer domain).

A uniform, temporally steady velocity profile was assumed at the inlet of the computational domain. The authors are not aware of any spatiotemporal turbulent intensity measurements in a tidal current stream. Thus we made the simplifying assumption that the turbulence intensity was 5% and uniform at the inlet of the computational domain. A pressure outlet boundary condition was applied at the outlet. To reduce flow recirculations on the far-field boundaries and to improve the stability of the numerical

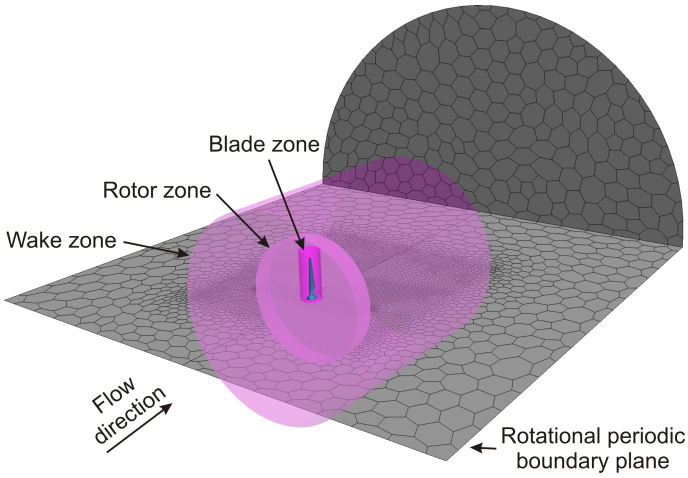

FIGURE 3. THE COMPUTATIONAL DOMAIN WITH GRID REFINEMENT REGIONS SHOWN.

solution, a slip (or symmetry) boundary condition was applied across the curved cylindrical surface of the outer domain. Lastly, a no-slip boundary condition was specified on all rotor surfaces.

Grid generation

The fidelity of any CFD simulation depends on the type of grid utilized (e.g. structured or unstructured) and the grid resolution. Structured hexahedral grids are the most desirable because they inherently provide highly accurate numerical solutions. As such, they have generally been used in CFD simulations of turbines. The downside of using structured grids is that the grid generation process is a manually intensive and time consuming task. In contrast, the creation of unstructured grids is a more automated process that can be performed in a fraction of the time. However, when using unstructured grids, care must be taken to insure the grid quality (e.g. grid element skewness, grid element aspect ratio, and grid density) does not adversely impact the accuracy of the numerical solution.

In the present study, unstructured grids consisting of polyhedral elements having an average of 14 faces per element were generated using the STAR CCM+ (CD-Acapco; Melville, New York) grid generation utility. The grid resolution was defined by specifying the grid size and expansion rate on all the surfaces of the computational domain. Additionally, we found it critical to use volumetric refinement zones to increase the grid resolution around the blade, the rotor, and in the wake region as shown in Fig. 3. These refinement zones allowed for the grid resolution to be increased in regions where high velocity gradients were expected, without adding additional grid elements in regions of the computational domain where a coarse grid was acceptable. Prism layer grid elements were extruded from the surfaces of the blade and the hub to improve the grid quality and control the grid

TABLE 2. COMPUTATIONAL GRID STATISTICS.

Grid #	Number of grid elements			Approx. grid resolution on blade (mm)	Approx. computational time for steady simulations (CPU-hours)
	Total	Turbine domain	Outer domain		
1	493378	4.00E+05	9.20E+04	85	6
2	1059090	8.60E+05	2.00E+05	64	50
3	3169642	2.60E+06	6.00E+05	43	150
4	5460348	4.50E+06	9.60E+05	36	300
5	11500527	9.40E+06	2.10E+06	28	640

spacing in this region. The height of the first prism layer was set so that the grid elements against the blade surface were within the logarithmic region of the boundary layer between y+ = 30 and y+ = 100, depending on the location of the grid element on the blade and on the turbine operating condition simulated. Wall functions derived from equilibrium turbulent boundary layer theory were utilized to model turbulent effects below the first grid cell.

Five grids were generated for use in the grid refinement and timestep studies. Table 2 summarizes the statistics for each grid and Fig. 4 illustrates the grid resolution achieved. Henceforth, the grids will be referred to by the grid number given in Tab. 2.

Numerical methods

The commercial CFD code STAR CCM+ was used to solve the incompressible Navier-Stokes equations using a second-order-accurate finite-volume discretization scheme via a segregated algebraic multi-grid iterative solver. A second-order-accurate backward temporal discretization was used for transient simulations.

Steady simulations were judged to be converged when the residuals of the numerical solution stabilized and were reduced by approximately three orders-of-magnitude. Several global parameters, including rotor torque and thrust, were also monitored to ensure convergence of the solution. Unsteady simulations were deemed converged when the average rotor torque over a revolution was within approximately 1% of the value from the previous revolution. Within each timestep, residuals were reduced by three orders-of-magnitude before the solution was advanced in time.

A rotating reference frame model was used to simulate the rotation of the blade and hub. This method simulates rotation without the need to physically rotate the computational grid by forming the governing equations for the rotor domain in a reference frame that rotates with the turbine, while the outer domain remains in a stationary coordinate system.

All simulations were performed on the 153 node Redrock computer cluster at the National Renewable Energy Laboratory. Each node is comprised of two 2.93 GHz quad-core Intel Nehalem processor with 12 GB of shared memory. All simulations

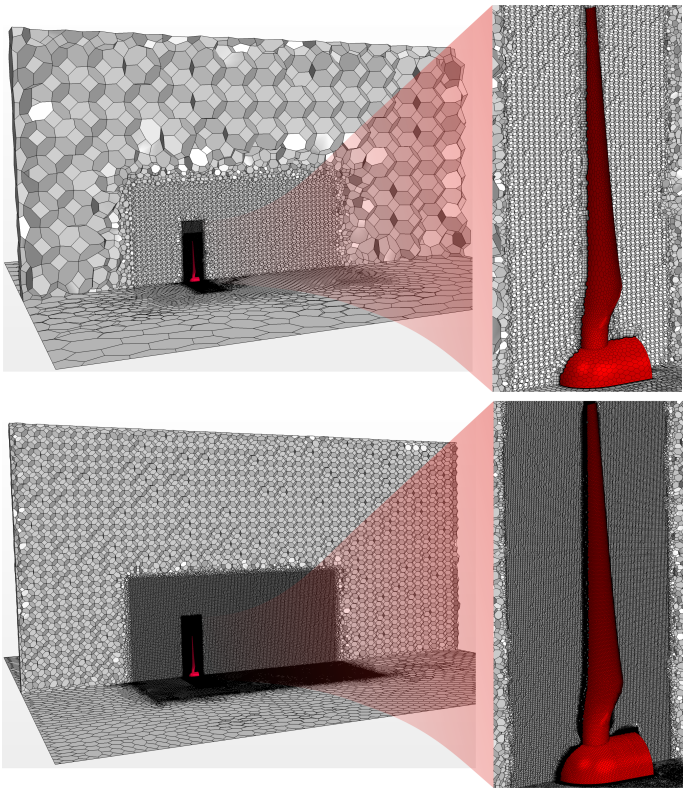

FIGURE 4. COMPARISON OF THE SPATIAL RESOLUTION ACHIEVED FOR (a) GRID 1 AND (b) GRID 5. THE RESOLUTION OF THE OTHER COMPUTATIONAL GRIDS FALLS BETWEEN THESE TWO EXTREMES.

TABLE 3. TURBINE OPERATION CONDITIONS SIMULATED WITH STAR CCM+. NOTE THAT THE ROTOR SPEEDS AND THE BLADE PITCH ANGLES FOR THE CORRESPONDING FLOW VELOCITIES WERE DETERMINED USING THE HARP_OPT DESIGN CODE.

Operating condition	Flow vel. (m/s)	Rotor spd. (rpm)	Blade pitch (deg)
A	1	6.68	0
B	1.5	10.03	0
C	1.9	11.5	0

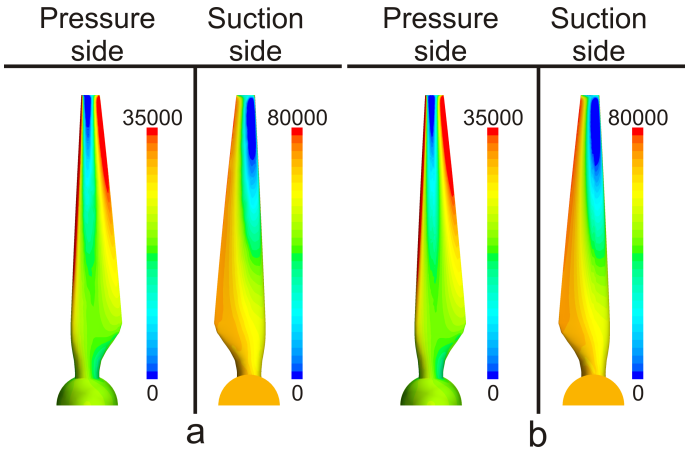

FIGURE 5. BLADE PRESSURE DISTRIBUTION IN PASCALS FOR (a) GRID 1 AND (b) GRID 5 FOR OPERATING CONDITION C.

were performed using 64 cores. Steady simulations required between 64 and 960 cpu-hours, depending on the grid size. Transient simulations were performed using grid 1 and required between 256 and 1500 cpu-hours, depending on the size of the computational timestep.

RESULTS AND DISCUSSION

Grid resolution study

The three turbine operating conditions presented in Tab. 3 were simulated under a steady flow assumption using each computational grid. The results from these simulations were used to study the influence of the grid resolution on the numerical solution. For brevity, graphical representations of the CFD solution (i.e. contour plots and iso-surfaces) will only be presented for grids 1 and 5, the coarsest and finest resolution grids, respectively.

Qualitatively, the features of the CFD solutions were found to be markedly similar for each grid. To illustrate the qualitative similarities between the solutions, examples of blade pressure distributions and velocity contours for operating condition C are presented in Figs. 5 and 6, respectively. Although the blade pressure distributions are nearly indistinguishable for the different grids, a close examination of the velocity contours reveals that small structures within the wake were better resolved using the higher resolution grid. A more diffuse wake region was predicted using grid 1 because the coarse grid cells in the wake region (see Fig. 4) were insufficient to resolve the shear layer between the turbine's wake and the free-stream flow. Note that the CFD results for operating conditions A and B exhibited similar qualitative trends to those shown in Figs. 5 and 6.

To quantitatively evaluate the effect of grid resolution on the numerical solution, the rotor torque and blade root flap moment were calculated for each grid. Figures 7 and 8 present these quantities plotted verses grid resolution for operating conditions A, B, and C. The relative differences between rotor torque and blade root flap moment predicted by grids 1–4 with respect to the value predicted using grid 5 are presented in Tab. 4.

As Fig. 7 illustrates, the CFD rotor torque predictions exhibited monotonic convergence with increasing grid resolution.

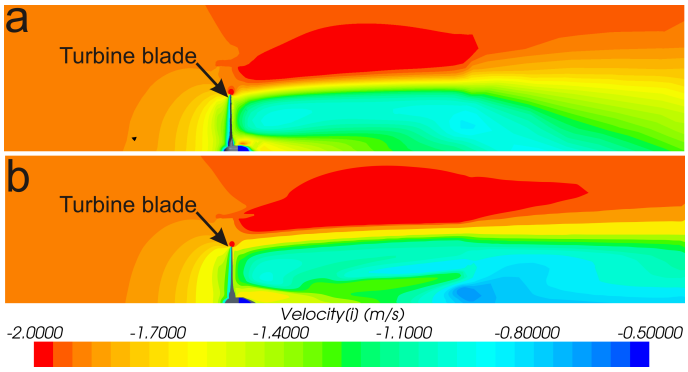

FIGURE 6. VELOCITY CONTOURS IN A PLANE THROUGH THE CENTER OF THE COMPUTATIONAL DOMAIN FOR (a) GRID 1 AND (b) GRID 5 FOR OPERATING CONDITION C. NOTE THAT THE FLOW IS FROM LEFT TO RIGHT.

TABLE 4. THE RELATIVE DIFFERENCE BETWEEN ROTOR TORQUE AND BLADE ROOT FLAP MOMENT PREDICTIONS MADE USING GRIDS 1-4 AND PREDICTIONS FROM GRID 5.

	Rotor torque difference (%)			Flap moment difference (%)		
Grid	Case A	Case B	Case C	Case A	Case B	Case C
1	-12.4	-12.7	-11.1	-0.9	-1.3	-1.2
2	-6.3	-6.9	-6.2	0.1	-0.3	-0.2
3	-2.7	-3.1	-2.7	0.3	0.1	0.1
4	-0.8	-1.1	-0.7	0.5	0.3	0.4

Moreover, torque predictions for grids 4 and 5 were within 1% of each other for all operating conditions simulated. Thus, based on these torque convergence data, it was concluded that further increasing the grid resolution would have produce a negligible change (almost certainly less than 1%) in the rotor torque predicted by CFD simulations. However, the results showed that use of a very coarse grid results in a significant under prediction of rotor torque. Indeed, as Tab. 4 shows, grid 1 consistently under predicted rotor torque by 11%–12% compared to grid 5.

To further investigate the cause of the discrepancy in the rotor torque predictions between the different grids, we computed the torque contribution from 40 evenly sized blade sections along the span. Figure 9 clearly shows that grid 1 significantly under predicted the rotor torque with respect to grid 5 on the outboard section of the blade, which was where the majority of the rotor torque was generated. This suggests that grid 1 had insufficient resolution to accurately capture the physical phenomena of the water flow over the outboard sections of the blade, where the

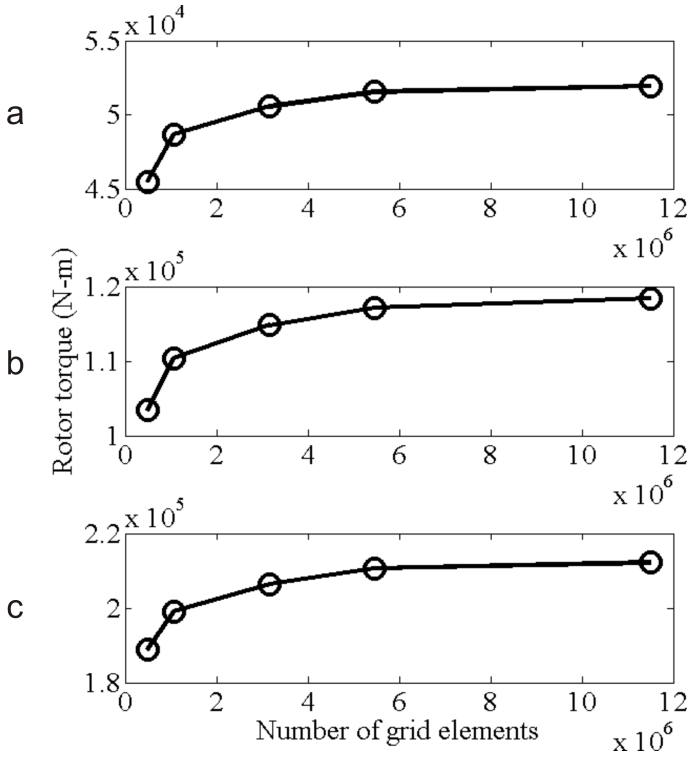

FIGURE 7. THE EFFECT OF GRID RESOLUTION ON ROTOR TORQUE PREDICTIONS FOR TURBINE OPERATION CONDITIONS (a) A, (b) B, AND (c) C.

relative flow velocity was highest.

One prominent difference between the predicted flow fields for grids 1 and 5 was visualized using iso-surfaces of vorticity to elucidate the blade tip-vortices. Figure 10 shows that the tip-vortices predicted by grid 1 were much larger and enveloped a larger portion of the blade than the tip-vortices predicted by grid 5. Effectively, grid 1 tip-vortices induced more downwash on the suction side of the blade, which decreased the torque generation near the blade tip as Fig. 9 clearly illustrates.

Predictions of the blade root flap moment were insensitive to the grid resolution (see Fig. 8 and Tab. 4), although the convergence of this quantity was not monotonic. Nevertheless, given that the maximum difference in the predicted flap moment between grids 1 and 5 was only 1.2%, this non-monotonic convergence was not of significant concern. One possible reason this convergence behavior was observed is that a steady flow assumption may not be appropriate for the highly unsteady far-wake region. More specifically, the near-wake region is characterized by a highly organized vortex wake with a structure that is effectively time-independent with respect to the rotating reference frame model. In contrast, the far-wake region is inherently unsteady regardless of the reference frame used.

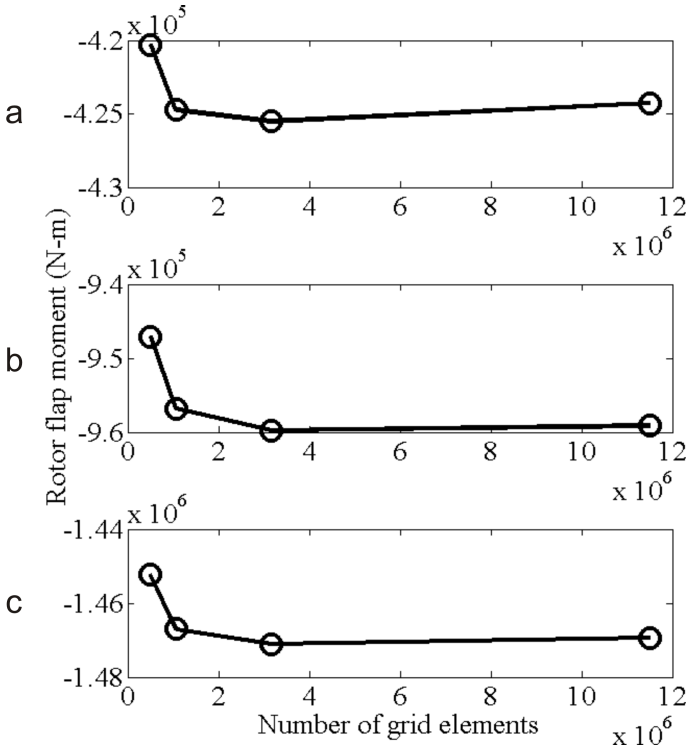

FIGURE 8. THE EFFECT OF GRID RESOLUTION ON BLADE ROOT FLAP MOMENT PREDICTIONS FOR TURBINE OPERATION CONDITIONS (a) A, (b) B, AND (c) C.

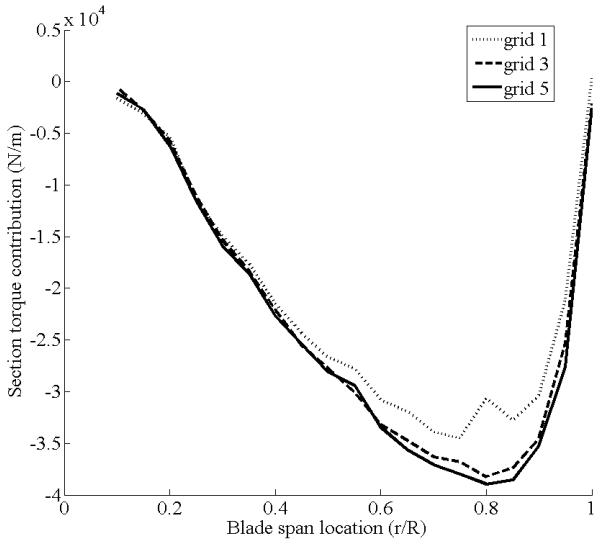

FIGURE 9. SECTIONAL TORQUE CONTRIBUTIONS FOR GRIDS 1, 3, AND 5.

Although a large difference in the predicted rotor torque (11–12%) was seen between grids 1 and 5, a less pronounced difference (approximately 3%) was observed between grids 3 and 5. Thus, if the purpose of CFD simulations is to accurately predict global turbine performance characteristics (e.g. rotor torque, flap moment, and hydrodynamic forces) a grid with a resolution similar to grid 3 appears sufficient. However, if fine details in the flow (e.g. the structure of tip vortices and details of the blade boundary layer and wake) must be resolved, a finer grid is required.

Timestep study

Transient simulations were performed for two reasons: (1) to determine if time-accurate CFD simulations provide significantly different results from corresponding steady simulations; and (2) to evaluate the effect of the computational timestep on the numerical solution. Grid 1 was used for all transient simulations to reduce the computational resources required to perform the timestep study. It is generally acceptable to use separate grid and timestep convergence studies to determine the effect of spatial and temporal resolution on CFD solutions [20]. Thus we expect the results from the timestep study using grid 1 to be applicable to transient simulations performed using the more resolved grids.

The transient simulations were performed using timesteps of 0.05, 0.01, and 0.005 seconds for operating condition C. These timesteps correspond 260, 521, and 1044 timesteps per rotor revolution, respectively. To reduce the required time for transient simulations to reach a quasi-steady state, the simulations were initialized using the steady flow solution. For all transient simulations, the torque stabilized within approximately three simulated rotor revolutions. Significant oscillations in the rotor torque were not observed and were not expected as the angle of attack of the blade over the entire span was well below the stall angle. Visualization of limiting streamlines on the blade confirmed the flow was fully attached.

The size of the computational timestep was found to have very little effect on the magnitude of torque generated by the turbine as Tab. 5 shows. Further, the difference between the torque predicted by the steady and unsteady simulations was within 2.5%. This suggests that for attached flow conditions, steady CFD simulations sufficiently captured the physical phenomena that determine the magnitude of hydrodynamic loading on the blade. This conclusion must, however, be considered carefully given the set of assumptions used for the present simulations. It was assumed the inflow conditions were spatiotemporally uniform. If a time-varying nonuniform velocity profile containing realistic turbulent structures is used, time-accurate simulations are required.

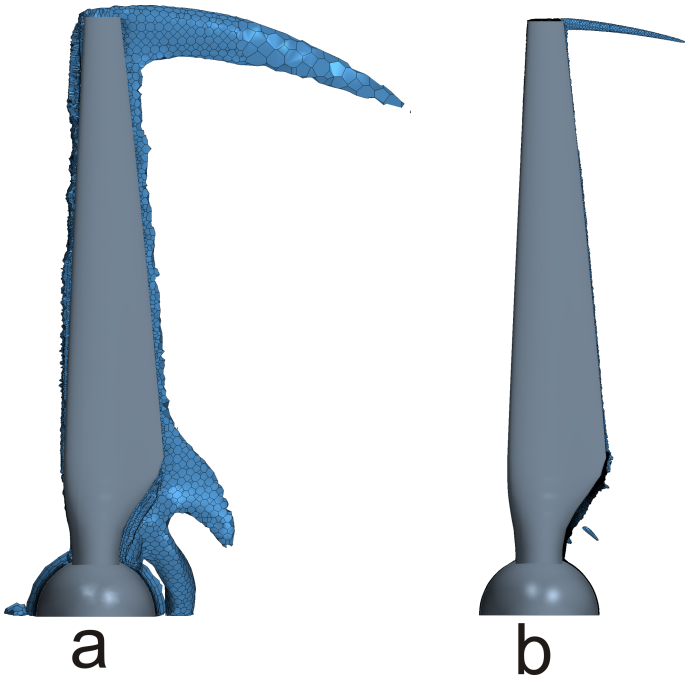

FIGURE 10. VISUALIZATION OF BLADE TIP-VORTICES FOR (a) GRID 1 AND (b) GRID 5. NOTE THAT THE SAME VORTEX THRESHOLD IS USED IN BOTH IMAGES.

TABLE 5. RESULTS FROM THE TIMESTEP STUDY. FOR COMPARISON, THE CORRESPONDING RESULT FROM THE STEADY SIMULATIONS IS ALSO SHOWN. NOTE THAT ALL RESULTS ARE FOR GRID 1.

Time-step (s)	Rotor torque (N-m)
Steady	1.89×10^5
0.05	1.91×10^5
0.01	1.93×10^5
0.005	1.94×10^5

Comparison of the CFD results with blade element momentum method predictions

The rotor torque and blade root flap moment predictions from steady CFD simulations performed using grid 5 were compared with the corresponding blade element momentum predictions from WT_Perf. Figure 11 presents this comparison. It is clear that the blade element momentum method significantly underestimated the hydrodynamic forces on the blade compared to the CFD solution. Indeed, plotting the sectional torque contributions to the total rotor torque (Fig. 12) revealed that the hydrodynamic forces were under predicted across the entire blade span by WT_Perf in comparison to the CFD solution. Unfortunately, there is no experimental data available for the current blade design, making it impossible to assess the accuracy of either numerical method. Nevertheless, the reasonable agreement between the CFD results and the blade element momentum method calculations provides confidence in the results obtained with both numerical methods.

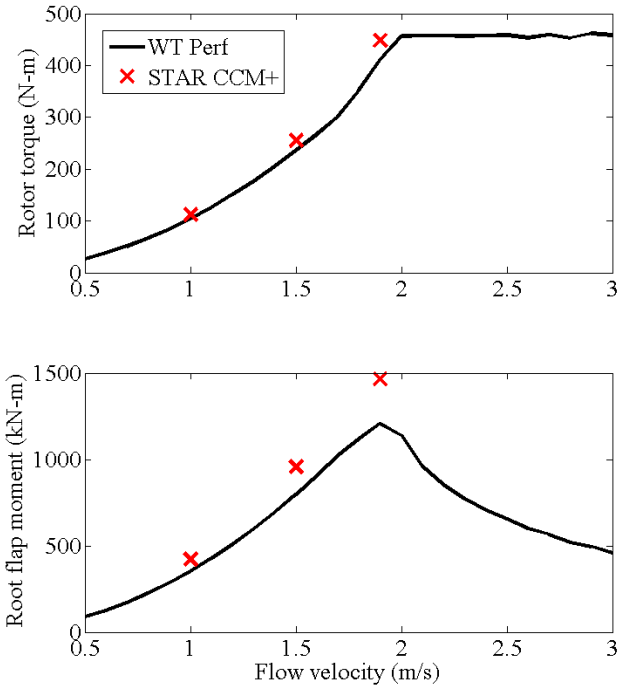

FIGURE 11. COMPARISON OF ROTOR TORQUE AND BLADE ROOT FLAP MOMENT PREDICTIONS FROM STAR CCM+ (USING GRID 5) AND WT_Perf FOR OPERATING CONDITION C.

CONCLUSIONS AND FUTURE WORK

A RANS CFD methodology to simulate HATTs was developed and the numerical results were verified via a grid refinement study and a timestep study. Steady simulations were performed using successively more resolved computational grids to determine the effect of grid resolution on CFD predictions. Qualitatively, the CFD solutions calculated using the different grids were markedly similar. However, the use of a coarse computational grid resulted in a significant under prediction of rotor torque compared to results obtained with higher resolution grids.

Transient simulations were performed using successively smaller computational timesteps to determine if temporal effects

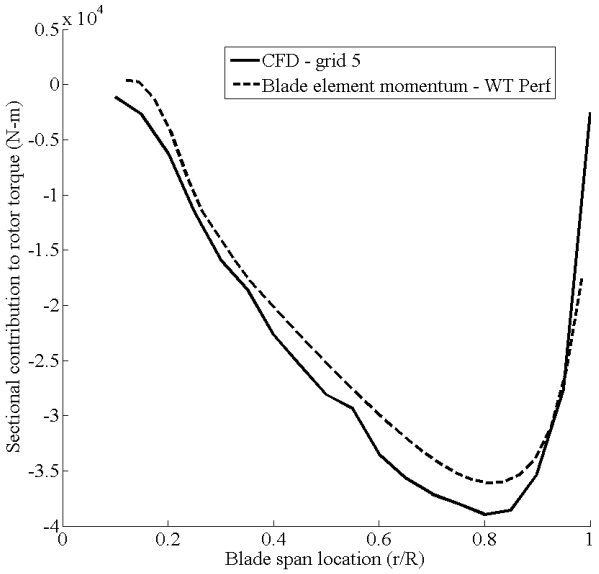

FIGURE 12. CONTRIBUTIONS TO ROTOR TORQUE PREDICTED USING CFD AND WT_Perf FOR OPERATING CONDITION C.

must be considered to make accurate predictions of turbine performance. For the turbine operating conditions considered, the computational timestep was shown to have little effect on the numerical solution. Additionally, the results from steady and transient simulation were shown to be in general agreement.

It is important to note that the flow over the turbine blade was fully attached for all the operating conditions simulated herein. The consideration of more extreme operating conditions, where the flow over the blades is separated and inherently unsteady, will likely require the use of transient CFD simulations to achieve accurate numerical results. Moreover, when the flow over the blades is separated, predictions of transition, separation, and flow reattachment have a significant influence on the accuracy of CFD solutions [8]. Thus, in these cases, advanced RANS models capable of predicting these complex physical phenomena may be required.

This work represents the first step in the development of a CFD methodology to characterize HATT performance. We plan to further develop this model by considering realistic inlet velocity profiles and turbulence levels. Additionally, we hope to include structural elements of the turbine, such as the tower and the nacelle, in future simulations.

ACKNOWLEDGMENT

We would like to acknowledge the U.S. Department of Energy Marine Hydrokinetic Energy Research Program for funding this work under agreement #21372. We also thank Robert Thresher for his general guidance and review of this work.

REFERENCES

[1] Fraenkel, P., 2002. "Power from marine currents". *Proceedings of the Institution of Mechanical Engineers, Part A: Journal of Power and Energy,* ***216***(1), pp. 1–14.

[2] Batten, W. M. J., Bahaj, A. S., Molland, A. F., and Chaplin, J. R., 2008. "The prediction of the hydrodynamic performance of marine current turbines". *Renewable Energy,* ***33***(5), pp. 1085–1096.

[3] Batten, W. M. J., Bahaj, A. S., Molland, A. F., Chaplin, J. R., and Sustainable Energy Res, G., 2007. "Experimentally validated numerical method for the hydrodynamic design of horizontal axis tidal turbines". *Ocean Engineering,* ***34***(7), pp. 1013–1020.

[4] Baltazar, J., and de Campos, J., 2008. "Hydrodynamic Analysis of Horizontal Axis Marine Current Turbine with a Boundary Element Method". Proceedings of the 27th International Conference on Offshore Mechanics and Arctic Engineering.

[5] Baltazar, J., and de Campos, J. A. C. F., 2009. "Unsteady analysis of a horizontal axis marine current turbine in yawed inflow conditions with a panel method". First International Symposium on Marine Propulsors.

[6] Bahaj, A., Batten, W., and McCann, G., 2007. "Experimental verifications of numerical predictions for the hydrodynamic performance of horizontal axis marine current turbines". *Renewable Energy,* ***32***(15), pp. 2479–2490.

[7] Bahaj, A., Molland, A., Chaplin, J., and Batten, W., 2007. "Power and thrust measurements of marine current turbines under various hydrodynamic flow conditions in a cavitation tunnel and a towing tank". *Renewable Energy,* ***32***(3), pp. 407–426.

[8] Pape, A., and Lecanu, J., 2004. "3D Navier–Stokes computations of a stall-regulated wind turbine". *Wind Energy,* ***7***(4), pp. 309–324.

[9] Sorensen, N., Michelsen, J., and Schreck, S., 2002. "Navier-stokes predictions of the NREL phase vi rotor in the NASA Ames 80 ft by 120 ft wind tunnel". *Wind Energy,* ***5***(2-3), pp. 151–169.

[10] Johansen, J., Sorensen, N., Michelsen, J., and Schreck, S., 2002. "Detached-eddy simulation of flow around the NREL Phase VI blade". *Wind Energy,* ***5***(2-3), pp. 185–197.

[11] Duque, E., Burklund, M., and Johnson, W., 2003. "Navier-Stokes and comprehensive analysis performance predictions of the NREL phase VI experiment". *Journal of Solar Energy Engineering,* ***125***, p. 457.

[12] Tongchitpakdee, C., Benjanirat, S., and Sankar, L., 2005. "Numerical simulation of the aerodynamics of horizontal

axis wind turbines under yawed flow conditions". *Journal of solar energy engineering,* ***127***, p. 464.

[13] Polagye, B., and Thomson, J., 2010. Tidal Energy Reference Model Inflow Conditions. Tech. Rep. Unpublished, University of Washington.

[14] Sale, D. C., and Li, Y., 2010. "Preliminary results from a design methodology and optimization code for horizontal axis wind and hydrokinetic turbines.". The 29th International Conference on Ocean, Offshore And Arctic Engineering.

[15] http://wind.nrel.gov/designcodes/simulators/wtperf/. NWTC Design Codes - WT_Perf, Accessed January 15, 2011.

[16] Menter, F., 1994. "Two-equation eddy-viscosity turbulence models for engineering applications". *AIAA journal,* ***32***(8), pp. 1598–1605.

[17] Laursen, J., Enevoldsen, P., and Hjort, S., 2007. "3D CFD quantification of the performance of a multi-megawatt wind turbine". In Journal of Physics: Conference Series, Vol. 75, IOP Publishing, p. 012007.

[18] Johansen, J., Madsen, H., Gaunaa, M., Bak, C., and Sørensen, N., 2009. "Design of a wind turbine rotor for maximum aerodynamic efficiency". *Wind Energy,* ***12***(3), pp. 261–273.

[19] Simms, D., 2001. NREL unsteady aerodynamics experiment in the NASA-Ames wind tunnel: a comparison of predictions to measurements. Tech. Rep. NREL/TP-500-29494, NREL.

[20] Roache, P. J., 1998. *Verification and Validation in Computational Science and Engineering*. Hermosa, Albuquerque, NM.